Observation and investigation of the ferrielectric subphase with high q_T parameter

Yu. P. Panarin, O. Kalinovskaya, and J. K. Vij*
Department of Electronic and Electrical Engineering, Trinity College, University of Dublin, Dublin 2, Ireland

J. W. Goodby
School of Chemistry, University of Hull, Hull, United Kingdom
(Received 17 June 1996; revised manuscript received 28 October 1996)

Dielectric relaxation processes in an antiferroelectric liquid crystal (AFLC) have been investigated over a wide range of frequencies from 1 Hz to 1 GHz. The AFLC under investigation possesses a variety of different ferrielectric, ferroelectric, and antiferroelectric phases. Dielectric and polarization measurements under direct bias voltage have been made with a view to clarifying the origin of the high-temperature ferrielectric phase, which appears between the AF and smectic-C^* phases. This phase is assigned to an unstable ferrielectric phase with q_T parameter greater than 1/2 (according to the Ising model) or a doubly modulated incommensurate phase (according to the expanded Landau model). The results are also supported by conoscopy. [S1063-651X(97)04704-1]

PACS number(s): 42.70.Df, 61.30.−v, 64.70.Md

I. INTRODUCTION

Although Beresnev *et al.* [1] proposed the existence of an antiferroelectric structure in a ferroelectric liquid crystal (FLC) mixture as early as 1982 to explain the unusual dependence of the pyroelectric properties on temperature, a detailed study of antiferroelectric liquid crystals (AFLCs) did not commence until Chandani *et al.* [2] in 1989 discovered the ability for tristable electro-optical switching. Later, from conoscopic investigations, various ferrielectric subphases were also discovered in the temperature range between the AFLC and the smectic-A (Sm-A) phases [3]. The appearance of these subphases can be understood to be a result of the competition between the antiferroelectric and ferroelectric interactions in adjacent smectic layers, which stabilize the Sm-C_A and the Sm-C^* phases. This competition produces various ferrielectric subphases with a different sequence of antiferroelectric (A) and ferroelectric (F) ordering among the smectic layers. Several different theoretical approaches have been advanced for explaining a variety of subphases and these postulates are based mostly on the expanded Landau model [4–6] or on the Ising model [7–9]. The double layered Landau model failed to explain the existence of some ferroelectric phases found experimentally, although it predicts the possibility of having some incommensurate phases [5]. The Ising model predicts the existence of an infinite number of ferrielectric phases. This model assumes an infinite number of interacting layers [7]. These ferrielectric phases, with varying temperature, can be characterized by the parameter $q_T(=m/n)$, denoting the fraction of ferroelectric ordering which appears in the antiferroelectric structure; n indicates the number of smectic layers and m is the number of ferroelectric orders within a period of the periodic structure. A complete set of ferrielectric subphases fills up the entire temperature range between Sm-C_A and Sm-C^* and these subphases are exhibited without any first-order transitions. Such a sequence is named a ''devil's staircase'' [7]. The stability of the phases with $q_T=m/n$ quickly decreases with the increase of number n. Although some of the ferrielectric phases with $q_T \leqslant 1/2$ and sufficiently high n (9 or even 11) were experimentally found [9], the existence of the phases with q_T higher that 1/2 had not been reported until Hatano *et al.* [10] observed some unusual ferrielectric phase between antiferroelectric AF ($q_T=1/2$) and ferroelectric Sm-C^* phases. According to the Ising model the q_T parameter of this phase must be between 1/2 and 1. An investigation of the structure of such a phase is the main focus of this study.

Detailed dielectric, electro-optic and pyroelectric data were given in previous investigations [9–13,20]. Nevertheless, the upper frequency up to which the measurements were reported
was limited to 10 MHz and some of the results given were not completely understood. One of the unusual results, so far, has been the observation of the two relaxation processes: ferrielectric and ferroelectric Goldstone modes coexisting over a wide range of temperatures corresponding to the Sm-C^* and/or Sm-C_γ phase [11–13]. The results of dielectric and electro-optical investigations of a AFLC sample over wide ranges of frequency and temperature now give answers to the aforesaid questions.

II. EXPERIMENT

We provide investigations of the AFLC sample under bias voltage for cells of thicknesses varying from 8 to 100 μm. The AFLC sample used in the experiments was AS-573 (Hull, UK) possessing the following structure and phase transition sequence [11] [defined by differential scanning calorimetry (DSC)]:

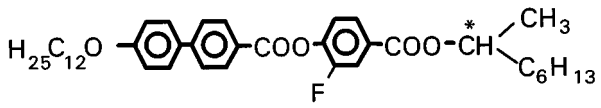

AS-573:Sm-C_A 78.3 Sm-C^*_γ 82 Sm-C^* 90.7 Sm-A 105.7 Is.

*Author for correspondence.

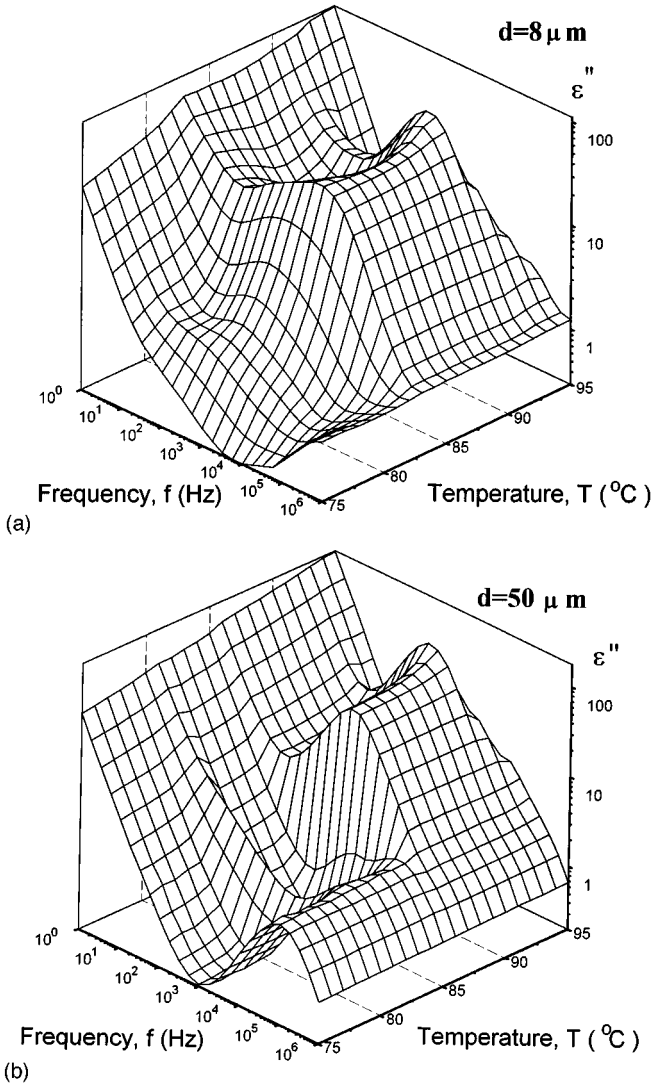

FIG. 1. Dielectric loss spectra vs temperature for AS-573, (a) $d=8$ μm, (b) $d=50$ μm.

Sample cells for low-frequency (<1 MHz) dielectric measurements consisted of indium tin oxide (ITO) coated glass plates with the low resistance of 30 Ω. The cells for high-frequency measurements (>1 MHz) were prepared using brass electrodes. For planar alignment, the conducting inner surfaces were spin coated with a polyvinyl alcohol (PVA) alignment layer and rubbed parallel. The cells were filled in the isotropic phase. Textures of experimental cells were observed using a polarizing microscope. Dielectric measurements in the frequency range from 1 Hz to 100 kHz were made using a Schlumberger 1255A frequency response analyzer and a Chelsea dielectric interface. In the higher frequency range we used Hewlett-Packard impedance analyzers: HP-4192A (10 kHz–10 MHz) and HP-4191A (10 MHz–1 GHz). During measurements, this system enabled us to superimpose direct bias voltages up to 40 V on a rms alternating voltage of 0.05 V.

For conoscopic measurements, homeotropically aligned cells of 160 μm thickness were used. Aluminum foil strips were used as electrodes and these were spaced apart by approximately a gap of 1 mm. Homeotropic alignment was produced by the aligning agent carboxylatochromium com-

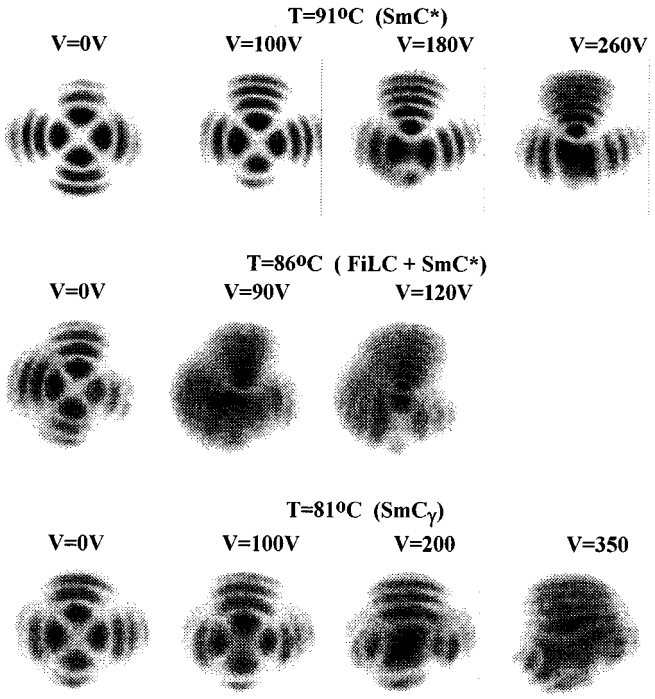

FIG. 2. Conoscopic pictures under bias voltage different phases: Sm-C^*, 91 °C; FiLC, 86 °C; Sm-C_γ, 81 °C.

plexes (chromolane) and used without rubbing. The spontaneous polarization was measured using the integral reversed current method [14].

III. RESULTS AND DISCUSSION

A. Determination of the phase transitions

The dielectric response of AFLC samples under dc bias fields in cells with cell thicknesses of 8, 20, 50, and 100 μm, was studied. Figure 1 presents the dependence of the dielectric loss spectra versus temperature in the absence of direct bias voltage for 8 μm and 50 μm cells. A comparison of these two plots reveals a remarkable dependence of a part of the spectra on the sample thickness. For a cell with the larger of the two thicknesses, we find that in the temperature range between Sm-C_γ and Sm-C^*, the dielectric spectra look similar to the spectra of an antiferroelectric phase, Sm-C_A. The experimental dielectric spectra are found to be practically independent of the cell thickness for cells thicker that 20 μm. We therefore conclude that in thin cells (with a thickness of the order of 8 μm or less) some of the ferrielectric subphases are suppressed by the surface interactions. Because the exact phase transitions sequence is very important to our study, we employed conoscopy and the spontaneous polarization measurements for obtaining information about the phase transitions.

Figure 2 presents the conoscopic pictures for homeotropic orientation for different temperatures and voltages. In the Sm-C^* phase ($T=91$ °C) an increase of the voltage shifts the center of the image in the direction perpendicular to the applied field and the center continues on shifting in this direction with an increase in voltage. The structure is getting increasingly biaxial with the optical plane continuing to be perpendicular to the direction of the applied field. Such behavior is typical of a ferroelectric Sm-C^* phase [3]. In the

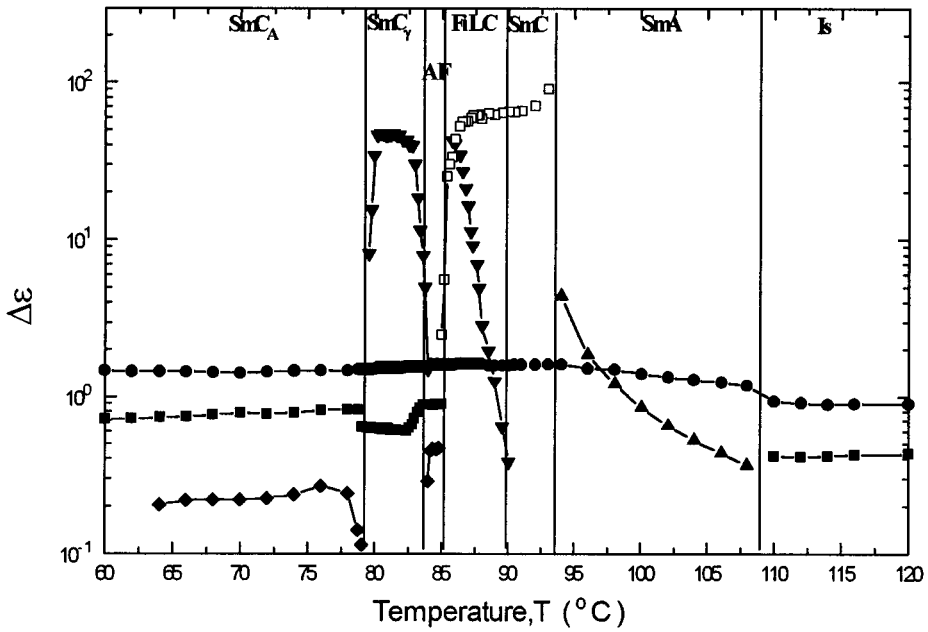

FIG. 3. Dependence of the dielectric strength ($\Delta\varepsilon$) on temperature for AS-573, $d=50$ μm.

Sm-C_γ phase (Fig. 2, $T=82$ °C) the dependence of the conoscopic image on voltage is similar to that of the Sm-C^* phase with only one difference. This is that the optical plane is parallel to the direction of the field, in contrast to being perpendicular to it. For a temperature range between 83 °C and 85 °C and less than 78 °C, the conoscopic pictures are typically antiferroelectric [3]. Therefore, we conclude that there exist a usual antiferroelectric phase Sm-C_A ($q_T=0$) at low temperatures and an antiferroelectric AF phase ($q_T=1/2$) at high temperatures. The unusual behavior was found in the temperature range from 85 °C to 90 °C. The application of a sufficiently low voltage makes the image rather blurred, although a detailed examination of the pictures reveals the existence of four centers: one pair as in the ferroelectric phase and another in the ferrielectric phase. Such an observation cannot possibly be made for a uniform structure. A further increase of the applied voltage makes the conoscopic image clearly ferroelectriclike. The identification of this phase will be discussed later, but here we just mention that, in this temperature range, there exist two different Goldstone type relaxation processes: ferroelectric and ferrielectric. Therefore we propose that in this temperature range there exist two phases Sm-C^* and some ferrielectric phase FiLC with $1/2<q_T<1$. This conclusion is supported by results of the dielectric and induced polarization investigations to be presented in the latter part of this paper. The full phase sequence of the sample is found to be as follows:

$$\mathrm{Sm}C_A\ 78.3\ \mathrm{Sm}C^*_\gamma\ 83.5\ \mathrm{AF}\ 85\ \mathrm{FiLC}\ 90\ \mathrm{Sm}C^*\ 93\ \mathrm{Sm}A\ 105.7\ \mathrm{Is}.$$

The phase sequences obtained from conoscopic pictures are significantly different from that originally produced by DSC. AF and FiLC were not revealed by DSC. Our conclusion with regard to the use of DSC therefore confirms that drawn in Ref. [10] that DSC cannot accurately detect phase transitions between some ferrielectric and antiferroelectric phases due to a finite hysteresis in temperature and a small change in enthalpy at the phase transitions.

B. Dielectric relaxations without bias field

The dielectric spectra are fitted to the Havriliak-Negami equation for n relaxation processes

$$\varepsilon^*(\omega)=\varepsilon_\infty+\sum_{j=1}^{n}\frac{\Delta\varepsilon_j}{[1+(i\omega\tau_j)^\alpha]^\beta}. \qquad (1)$$

$\varepsilon^*(\omega)$ is the frequency dependent complex permittivity, ε_∞ is the high-frequency permittivity, j is a variable denoting the number of the relaxation processes up to n, τ_j is the relaxation time of jth relaxation process, α and β are the fitting parameters, and $\Delta\varepsilon_j$ is the dielectric relaxation strength (or the static susceptibility, χ_j) for the jth process.

Figures 3 and 4 present the temperature dependence of the dielectric parameters of AS-573. These are found by fitting the dielectric spectra to the Havriliak-Negami equation using a fitting program DK36 developed in Mainz.

1. Molecular relaxation processes.

At temperatures corresponding to the isotropic phase, we observe two noncollective (molecular) relaxation processes. The higher-frequency process is assigned to the molecular relaxation around the long molecular axis and the lower-frequency process is that around the short axis. It follows

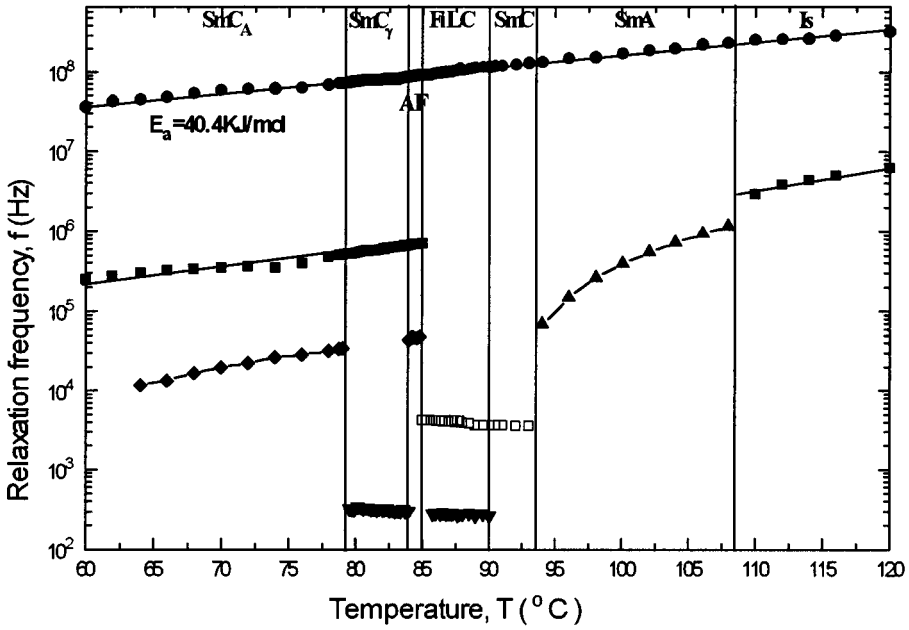

FIG. 4. Dependence of the relaxation frequency (f) on temperature for AS-573 $d=50$ μm; the temperature range is divided up into the various phases.

from the fact that in the Sm-A phase, the molecules being parallel to the plane of the electrodes, there exist only the higher-frequency relaxation process and the soft mode. The results presented in Figs. 3 and 4 show that the relaxation frequencies of both molecular processes are Arrhenius; however, the dielectric strengths possess complicated behavior. To explain this phenomenon we introduce some geometric factors which affect the dielectric strength of the molecular relaxation processes. For the simplest cases of the planar or homeotropic alignments, it is obvious that there exist only one of the two molecular relaxation processes.

Let us assume that the long molecular axis makes an angle ϑ, with respect to the plane of the electrodes, as shown at the Fig. 5. The dipole moment $\boldsymbol{\mu}$ has a component along the long molecular axis $\boldsymbol{\mu}_l$ and the transverse component $\boldsymbol{\mu}_t$ such that $\boldsymbol{\mu}=\boldsymbol{\mu}_t+\boldsymbol{\mu}_l$. The application of the electric field will bias the dipolar rotation and induce polarization along (P_l) and perpendicular (P_t) to the long molecular axis, respectively. The static susceptibility χ_S of the β relaxation for rotation around the short axis (β_S) that appears along the direction of the electric field depends on angle ϑ through the following equation:

$$\chi_s(\vartheta)=\left.\frac{\vec{P}_l}{\vec{E}}\right|_X=\left.\frac{P_l\sin\vartheta}{E}\right|_X=\frac{P_l}{E}\sin^2\vartheta=\chi_{s0}\sin^2\vartheta, \quad (2)$$

where χ_{s0} is the maximum dielectric susceptibility of the β relaxation for a rotation around the short axis and this alone can be found from the homeotropic configuration. One power of sin ϑ arises from the projection of the electric field on the long molecular axis, and the second power arises from the projection of the induced polarization on to the surface normal or the X axis.

For the static susceptibility χ_l of the β relaxation for rotation around long axis (β_l) we can similarly write

$$\chi_l(\vartheta)=\chi_{l0}\cos^2\vartheta, \quad (3)$$

where χ_{l0} is the maximum static susceptibility of the β relaxation for rotation around the long axis and can be found for the planar orientation.

These equations predict the existence of both molecular relaxation modes in the isotropic phase, since ϑ is arbitrarily distributed and only the molecular relaxation around the short axis in the Sm-A phase can be seen, because all the molecules are aligned parallel to the electrodes ($\vartheta=0$). This is in agreement with the experimental results presented in Figs. 3 and 4.

For a cell in the bookshelf structure, the angle ϑ can be found from the following geometric expression (see Fig. 6):

$$\sin\vartheta=\sin\theta\,\sin\varphi, \quad (4)$$

where φ is the azimuthal angle between the C director and the Y axis and θ are the smectic tilt angles. For small angles, i.e., $\theta<1$, Eqs. (3) and (4) can be simplified as follows:

$$\vartheta(\varphi)=\theta\,\sin\varphi, \quad (5)$$

$$\chi_l(\vartheta)=\chi_{l0}\cos^2\vartheta=\chi_{l0}(1-\sin^2\vartheta)=\chi_{l0}(1-\vartheta^2). \quad (6)$$

On integrating this equation over the helical pitch we can find the average susceptibility $\widetilde{\chi}_l$

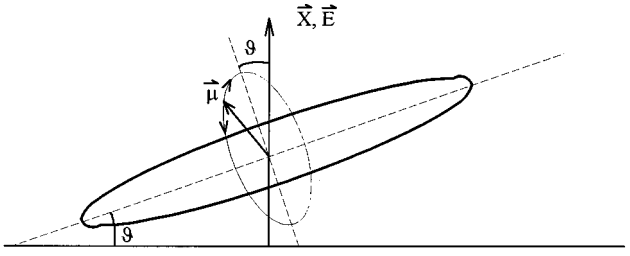

FIG. 5. Molecular orientation in the cell; ϑ is the glass plate; $\vec{\mu}$ is the molecular dipole moment.

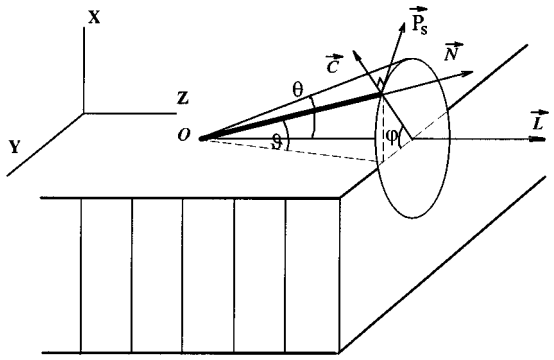

FIG. 6. Smectic layer structure for a bookshelf cell. (X,Y,Z) is the coordinate system, N is the molecular director, L is the smectic layer normal, C is the c director, θ is the tilt angle, ϑ is the angle between molecular director and the electrode plane, and φ is the azimuthal angle; the plane YZ is that of the glass plate.

$$\tilde{\chi}_l=\frac{1}{p_0}\int_0^{p_0}\chi_{l0}[1-\vartheta^2(z)]dz$$

$$=\chi_{l0}-\frac{1}{p_0}\int_0^{p_0}\chi_{l0}\vartheta^2(z)dz, \tag{7}$$

for an *undisturbed* helical structure we can write

$$\varphi=\frac{2\pi z}{p_0}, \quad z=\frac{\varphi p_0}{2\pi}$$

and

$$\tilde{\chi}_l=\chi_{l0}-\frac{1}{2\pi}\int_0^{2\pi}\chi_{l0}\vartheta^2(\varphi)d\varphi$$

$$=\chi_{l0}-\frac{1}{2\pi}\int_0^{2\pi}\chi_{l0}\theta^2\sin^2\varphi\ d\varphi=\chi_{l0}\left(1-\frac{\theta^2}{2}\right). \tag{8}$$

Therefore the dielectric strength for the high-frequency molecular relaxation in the helical phase is lower than in the unwound Sm-C^* structure by $\theta^2/2$. This is in agreement with the experimental data (Fig. 3). For the helical structure, the dielectric susceptibility due to rotation around the short axis is found to be as follows:

$$\tilde{\chi}_s=\frac{1}{p_0}\int_0^{p_0}\chi_{s0}\ \sin^2[\vartheta(z)]dz=\chi_{s0}\ \frac{\theta^2}{2}. \tag{9}$$

It means that for helical structures as in Sm-C^*, Sm-C_γ, and Sm-C_A we can observe the molecular relaxation around the short axis.

We thus find that the dielectric strengths for both molecular dynamical processes are sensitive to the average angle between the molecular director and the surface of the electrodes, and this formalism can be used as the basis for determining the molecular structure present in the cell.

2. Collective relaxation processes in the ferrielectric phases.

In the Sm-C^* phase and at temperatures of several degrees below the Sm-A–Sm-C^* phase transition, there exist two relaxation processes: molecular relaxation around the long molecular axis and the ferroelectric Goldstone mode. One could also expect the molecular relaxation around the short molecular axis to exist because some molecules are no longer perpendicular to the electric field because of the existence of a helical Sm-C^* structure. These molecular processes are, however, undetectable due to a superposition of an intense Goldstone mode on to the molecular modes. On decreasing the temperature, the second relaxation process has already been reported [12,13] to gradually show up in the dielectric spectra in the temperature range from 90 °C to 85 °C. In addition to the ferroelectric Goldstone process discussed above, another relaxation process appears 3 °C below the Sm-C^*–Sm-A phase transition. This process seems to be the ferrielectric Goldstone mode because its frequency is almost of the same value as that of the ferrielectric Goldstone mode in the Sm-C^*_γ phase (Fig. 4). In the usual ferrielectric Sm-C^*_γ phase, there exists only one ferrielectric Goldstone mode. The relaxation frequency of this process is in agreement with the phenomenological theory developed by Cepič *et al.* [18], which describes the dynamical behavior and the dielectric spectra of different Sm-$C_A(q_T)$ subphases. According to this model the relaxation frequency of the Goldstone mode below the phase transition temperature Sm-$C^*\rightarrow$Sm-C^*_γ decreases by approximately one order of magnitude and the dielectric strength increases by several orders. This behavior was observed experimentally in MHPOBC [15]. In our case the relaxation frequencies of the Goldstone modes in ferrielectric and ferroelectric phases also differ by approximately one order of magnitude.

As mentioned above, the main interest in this section of the paper lies in the coexistence of two relaxation processes in the temperature range that corresponds (according to DSC data) to the Sm-C^* phase. According to the temperature induced devil's staircase model [9] the q_T parameter always increases with temperature. For the sample under investigation, in the lower-temperature range (<85 °C), there exist the antiferroelectric Sm-C_A phase ($q_T=0$), the ferrielectric phase ($q_T=1/3$), and the antiferroelectric AF phase ($q_T=1/2$). At higher temperatures, one could expect some ferrielectric phase ($1/2<q_T<1$) and/or ferroelectric Sm-C^* ($q_T=1$). At the same time the low-frequency relaxation process in the temperature range from 85 °C to 90 °C (Figs. 3 and 4) is of the same relaxation frequency as the ferrielectric Goldstone relaxation process in the Sm-C^*_γ phase. Thus we could reasonably expect the existence of some ferrielectric phase with $1/2<q_T<1$. From another point of view, there must be only one Goldstone mode seen in the ferrielectric phase. Therefore, the coexistence of two Goldstone relaxation processes at the same temperature could be explained by the existence of a mixture of domains of two different subphases (ferrielectric and ferroelectric), which is also supported by conoscopy. The relaxation processes in the antiferroelectric phases are also presented in Figs. 3 and 4; however, the mechanism of these will be discussed elsewhere.

C. Effect of bias voltage on the properties of the ferrielectric phases

The effect of bias voltage on the dielectric spectra in the Sm-C^*, Sm-C^*_γ, and Sm-C_A phases is similar to the results reported in the literature [15–19]. The application of the bias voltage to the FiLC phase considerably changes the dielectric spectra (Fig. 7). An increase in the bias voltage sup-

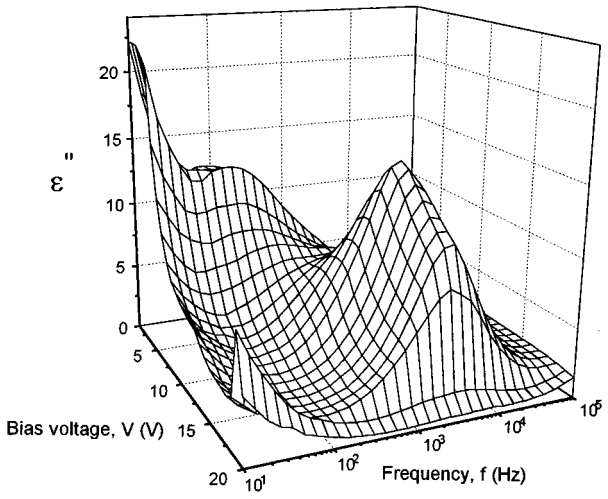

FIG. 7. Dielectric loss spectra vs bias voltage for the 50 μm cell in the FiLC phase, $T=86$ °C.

presses the low-frequency relaxation mode and causes an amplitude of the high-frequency process initially to increase and then to decrease with an increase in the bias voltage (Fig. 8). The value of the relaxation frequency of the low-frequency mode is the same as for the Goldstone mode in the ferrielectric Sm-C_γ^* phase, while the relaxation frequency of the high-frequency mode is the same as for the ferroelectric Goldstone mode (Fig. 4). Hence, these relaxation processes are denoted as ferrielectric and ferroelectric Goldstone modes. This phenomenon could be explained by taking into account the results of the conoscopic investigations presented in Fig. 2. If we suggest the coexistence of two phases FiLC and Sm-C^* in this temperature range, then at small electric fields we have two dielectric relaxation processes, and the mixture of two different conoscopic images, which leads to a complicated conoscopic picture (Fig. 2) already discussed. An application of the electric field would cause the transition from FiLC to Sm-C^*. This will cause a suppression of the ferrielectric mode in the dielectric spectra (Fig. 8) and an increase in the ferroelectric mode. At these voltages conoscopic pictures become ''ferroelectriclike.'' A further increase of the electric field will unwind the helix and suppress the ferroelectric Goldstone mode.

An application of the bias voltage in this FiLC phase causes the most interesting dependencies of the spontaneous polarization and that of the apparent tilt angle on the applied voltage, as shown in Fig. 9. For voltages in the range 5–30 V, there exists a field induced quasistable state with a sufficiently stable and high value (60–80 %) of the induced polarization and the tilt angle. Such high values of spontaneous polarization could be assigned to two possible structures: (i) the field induced devil's staircase (with $q_E=4/5$ or more) or (ii) the distorted ferroelectric helical structure. The experimental results discussed before support the second possibility. For example, the dielectric spectra in this state under bias voltage are typically ''ferroelectriclike'' and the relaxation frequency of the Goldstone mode is of a magnitude similar to the ferroelectric Sm-C^* phase. In this electric-field range, the conoscopic pictures show the existence of a ferroelectric helix (Fig. 2, $T=87$ °C, $V=120$ V).

According to the conventional model for the field induced devil's staircase all the molecules under applied voltage are parallel to the electrodes plane and the dielectric strength of molecular relaxation is maximal. For the distorted helical ferroelectric structure some molecules are not parallel to that plane. Therefore, a comparison of the results of the induced polarization with those of the dielectric strength for the high-frequency molecular relaxation mode under direct bias voltage would clarify the molecular structure. We chose the relaxation process around the long molecular axis because it possesses a high relaxation frequency and could be easily separated from other relaxation modes.

Figures 9 and 10 show the dependence of the normalized macroscopic polarization $P(V)/P_s$ and dielectric strength of the high-frequency molecular relaxation process as a function of the direct bias voltage for different temperatures (i.e., different phases).

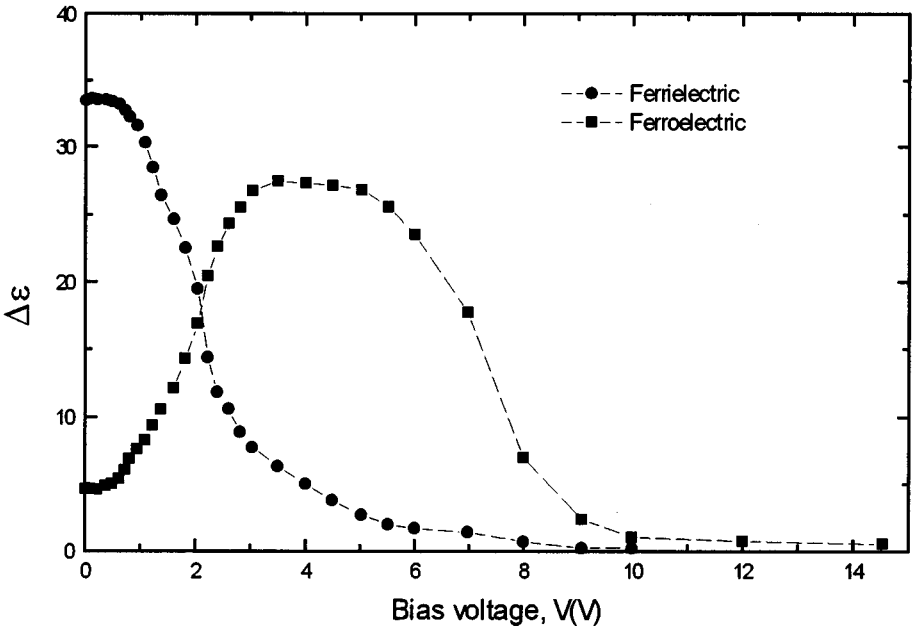

FIG. 8. Dielectric strength vs bias voltage for the low-frequency (ferrielectric) relaxation process and higher-frequency (ferroelectric) relaxation process at $T=86$ °C. The cell thickness is 50 μm.

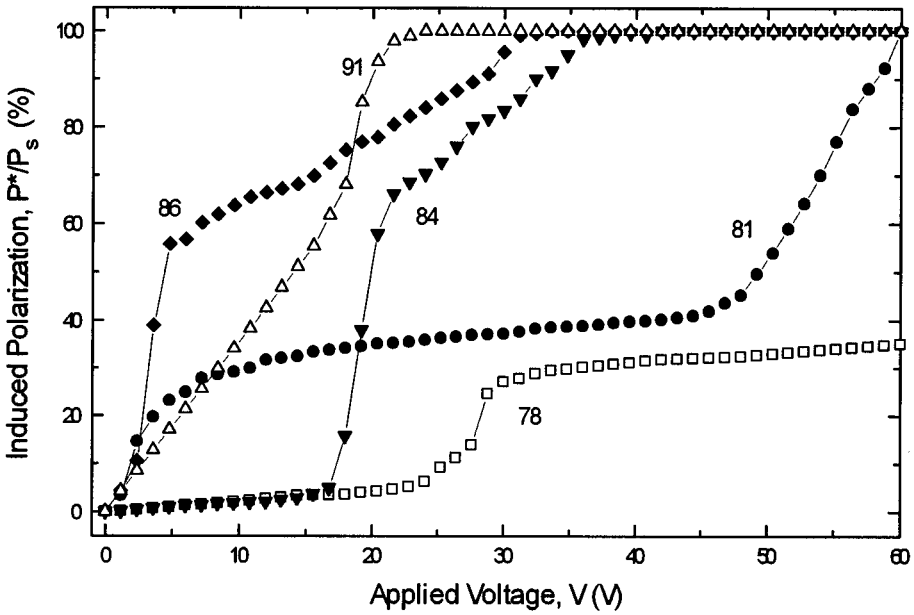

FIG. 9. Temperature dependence of the normalized spontaneous polarization as function of bias voltage for different phases: Sm-C^*, 91 °C; FiLC, 86 °C; AF 84 °C; Sm-C^*_γ-81 °C; Sm-C_A, 78 °C. The cell thickness is 50 μm.

At a temperature of 78 °C, which corresponds to the Sm-C_A phase, the macroscopic polarization is extremely low and almost independent of voltage until a threshold value in the region of 27–30 V is reached. At this voltage, the antiferroelectric structure changes to the ferrielectric ($q_E=2/3$) with an induced polarization of $\frac{1}{3}P_s$, in agreement with the field induced devil's staircase model. At the higher voltage (not shown in Fig. 9), the ferrielectric structure starts getting unwound and the macroscopic polarization reaches a saturation value of P_s. It is very important to note that the dielectric strength of the molecular relaxation (Fig. 10) does not follow the induced polarization plot but reaches a maximal saturation value at 35 V, for the voltage necessary to produce a field induced unwound Sm-C^*_γ phase. It is easily explainable as in both structures: in unwound ferrielectric ($q_E=2/3$) and unwound ferroelectric ($q_E=1$) all of the molecules lie in a plane of the electrodes and the dielectric strength is the same and of maximal value.

The polarization plot corresponding to the Sm-C^*_γ phase (81 °C) also shows typical ferrielectric dependence on voltage. For voltages in the range (0 V$<V<$5 V) polarization obeys almost linear dependence on voltage, corresponding to a distortion of the helix with voltage; then a saturation value of $P_s/3$ for an unwound ferrielectric structure ($q_E=2/3$) is reached. Finally at high voltages (60 V), not shown in Fig. 9, the macroscopic polarization reaches a saturation value of P_s. For this phase we find that the dielectric strength of the molecular relaxation reaches a maximal saturation value at 15–20 V (Fig. 10) when the induced polarization becomes $P_s/3$ and $q_E=2/3$. This is again understandable, as the molecules in the unwound ferrielectric state with $q_E=2/3$ are parallel to the plane of the electrodes.

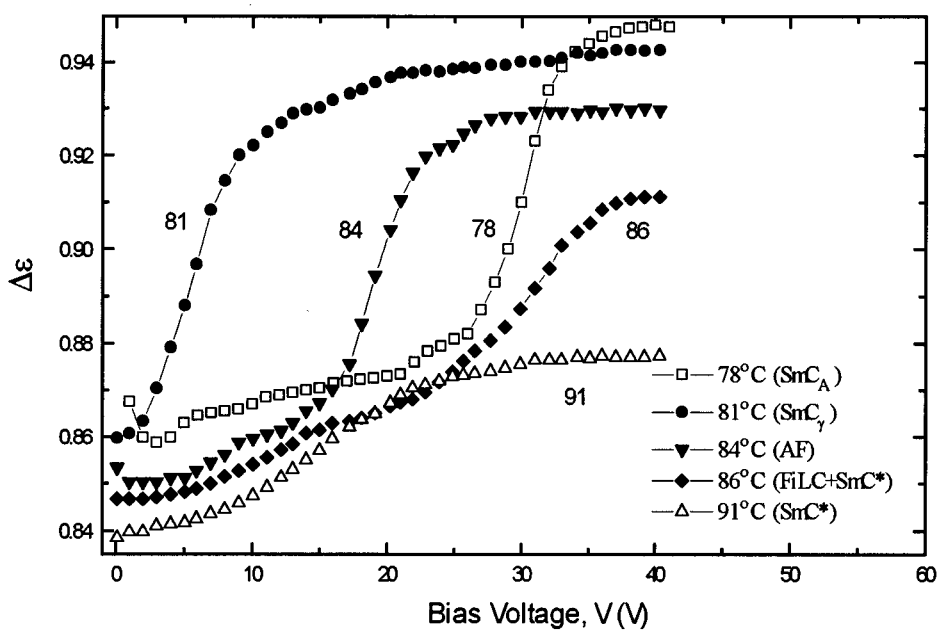

FIG. 10. Temperature dependence of the dielectric strength of the high-frequency molecular relaxation as function of bias voltage for different phases: Sm-C^*, 91 °C; FiLC, 86 °C; AF, 84 °C; Sm-C^*_γ, 81 °C; Sm-C_A, 78 °C. The cell thickness is 50 μm.

It should be mentioned here that currently some doubts about the validity of the Ising model and its modified, axial next-nearest-neighbor Ising (ANNNI) model for describing the molecular structure in the antiferroelectric and ferrielectric phases (see, for example, Ref. [6]) have been expressed. Nevertheless, the experimental results for Sm-C_A ($T=78$ °C) and Sm-C^*_γ ($T=81$ °C), which are presented in the two previous paragraphs, are well explained by the Ising model. It means that under a certain bias voltage the molecular structures that are attained with $q_E=2/3$ and an induced polarization P_s value of 1/3 have all their molecules lying parallel to the plane of the electrodes.

For the Sm-C^* phase ($T=91$ °C), the curve also shows a typical dependence of polarization on voltage for a helical Sm-C^* cell. For low voltages, the effective polarization and the dielectric strength are found to gradually increase with an increase in voltage and this corresponds to a distortion of the helix. At higher voltages the normalized polarization and the dielectric strength together reach a saturation value for the unwound Sm-C^* structure. Note that the results presented in Fig. 10 are in agreement with Eq. (8) for the dielectric strength of a molecular relaxation process around the long axis. Thus for the temperature range mentioned above, a dependence of the effective polarization and dielectric strength on voltage shows typical behavior for both Sm-C_A and Sm-C_γ phases. We emphasize again that in the unwound ferrielectric Sm-C^*_γ phase with an induced polarization of $P_s/3$, the dielectric strength of the molecular relaxation process reaches the maximal value in both Sm-C_A and Sm-C^*_γ phases.

Nevertheless, for the temperature range 85–90 °C (where we assume the existence of a FiLC phase) the macroscopic polarization (as well as the conoscopic pictures and the dielectric spectra) possess some interesting features. The dependence of the effective polarization on the bias voltage consists of two almost linear dependencies with different slopes (Fig. 9, $T=86$ °C). For a low bias voltage (0–5 V), the macroscopic polarization grows quickly with voltage and reaches a value equal to 60% of P_s. This process is accompanied by a decrease in the ferrielectric relaxation strength (Fig. 8) and a perturbation in the conoscopic image (Fig. 2). These observed effects can be explained by a model which involves a gradual change from a ferrielectric FiLC phase to the ferroelectric one with an increase of the bias voltage. When the entire FiLC phase is transformed to Sm-C^* ($\approx$30 V), the conoscopic image again gets sharper and ''ferroelectriclike'' (Fig. 2, $T=86$ °C, $V=120$ V). The dielectric spectrum at that stage exhibits only the ferroelectric Goldstone mode (Fig. 8) and thus the effective polarization grows gradually with voltage as the helix is strongly being deformed with an increase in the electric field. It was already mentioned that this state, with the effective polarization of 60–90 % P_s, could have been assigned to a step in the field induced devil's staircase. In that case, the dielectric strength of the molecular relaxation around the long axis, according to Eq. (8), must have a maximal value, as in the case of Sm-C^*_γ and Sm-C_A (Figs. 9, 10) but this is contrary to the observations. For the temperature range 85 °C–90 °C the dielectric strength of the molecular mode reaches a maximal value at the same threshold voltage at which the effective polarization reaches a saturation value of P_s, the helix is unwound, and the Goldstone mode is almost suppressed. Therefore, we conclude that this field induced quasistable level corresponds to that of the distorted ferroelectric helix and not to the field induced devil's staircase.

IV. COMPARISON OF DIFFERENT THEORETICAL MODELS WITH POSSIBLE MOLECULAR STRUCTURES

It has been shown that the AFLC sample under investigation in a temperature range (85 °C–90 °C) reveals unusual but interesting properties; these cannot be totally explained by the current theories which describe both a temperature induced and field induced ''devil's staircase'' observed in antiferroelectric and ferrielectric phases. The main points of disagreement are as follows: (i) Dielectric loss spectra consist of both ferroelectric and ferrielectric Goldstone relaxation modes.

(ii) Conoscopic images get blurred under relatively low bias fields and then these become clearly ferroelectriclike with an increase of the bias field.

(iii) A plot of the dependence of the effective polarization on the bias voltage consists of two almost linear parts with different slope.

(iv) There is no so-called field induced devil's staircase with a sufficiently stable level of induced polarization-tilt angle (1/9, 1/5, and/or 1/3) which has been observed at lower-temperature ferrielectric and antiferroelectric phases, such as Sm-C_A, Sm-C^*_γ, and AF.

(v) The dependence of the dielectric strength of the molecular relaxation mode around the long axis reaches the maximal value at the same voltage as does the effective polarization.

We give the two most probable explanations for these observed effects in a ferrielectric mesophase using the Ising (ANNNI) model and the expanded (bilayered) Landau model. The conclusion which is being arrived at from two different models is essentially the same.

From the Ising model, this phase exists between AF ($q_T=1/2$) and Sm-C^* ($q_T=1$) and according to the temperature induced devil's staircase the q_T parameter lying in the range from 1/2 to 1. This conclusion has been made by Hatano *et al.* [10] about the sample with a similar molecular structure (the nonchiral tail does not contain any oxygen, as in this case). The experimental investigation shows that this phase seems to be a thermodynamically unstable one. According to the numerous experimental investigations the Ising model is successful in describing the temperature induced devil's staircase for ferrielectric or antiferroelectric phases with $q_T \leqslant 1/2$. In such structures the ferroelectric ordering (F) appears as defects in the antiferroelectric structure $AAAA$. Ferroelectric orderings (F) repel each other due to Coulomb interactions. Such forces stabilize the equidistant arrangement of F ordering in the $AAAA$ matrix. In the phases with $q_T>1/2$ we have an opposite situation, namely, A ordering appears as defects in the $FFFF$ orderings. ''For such a structure, what is important for its stable existence is the repulsive forces between A orderings,..., it is not clear whether A orderings repel one another.'' [9] Consider, for example, the FiLC mesophase with $q_T=3/5$. Such a phase possesses the following arrangement: $\cdots FFAFA/FFAFA/FFAFA\cdots$. The two neighboring ferroelectric orderings repel each other and the arrangement $/FFAFA/$ possesses the

same electrostatic energy as /*FAFFA*/. The total arrangement could be: $\cdots FAFFA/FFAFA/FAFFA/FFAFA/FFAFA/FAFFA\cdots$ which possesses no stable period of structure. Therefore, this mesophase with $q_T>1/2$ could be considerably disturbed by the fluctuation forces and these could easily be affected by the external electric field as observed in our investigations. The same situation is valid for all the phases with $q_T>1/2$. Taking into account these considerations, we implicitly restrict the range of stable ferrielectric and antiferroelectric mesophases by the q_T parameter from 0 to 1/2.

The same conclusion follows explicitly from the expanded Landau model [4]. Žekš and Čepič [5] introduced Lifshitz invariants for the chiral systems and obtained 12 possible sequences of phase transitions between different ferrielectric and antiferroelectric phases. They predicted the existence of incommensurate doubly modulated phases lying in between the commonly known mesophases and, particularly, between Sm-C_γ^* and Sm-C^*. They did not investigate the effect of the direct electric field on these phases, but the coexistence of the two Goldstone relaxation processes (ferrielectric and ferroelectric) follows directly from the nature of these doubly modulated phases [5].

On assuming these explanations from two different points of view, the ferrielectric phase under investigation could be assigned as a thermodynamically unstable FiLC phase with $q_T>1/2$ or an incommensurate doubly modulated phase.

Finally, we remark about the validity of the two major theoretical approaches (the Ising and the expanded Landau) to describe the properties of AFLCs. The Ising model explains quite well the existence of and transformations between all experimentally found subphases with a temperature and electric field for phases with $q_T\leqslant 1/2$. For higher values of q_T, the discussion that has preceded should be taken into account. This inability of the Ising model to explain the observations in full arises from the chirality factors having been ignored in its formulation. The expanded Landau model with Lifshitz invariants properly explains the dielectric properties [18], phase transitions with temperature and the existence of the doubly modulated incommensurate subphases. The existence of some ferrielectric and antiferroelectric mesophases including experimentally found Fi_H, Fi_L, and AF can possibly be explained by taking into account higher degrees in the expression for the Landau free energy expansion.

V. CONCLUSIONS

A FiLC phase with $q_T>1/2$ has been observed. It is found that this phase is either thermodynamically unstable or is an incommensurate doubly modulated phase. The phase transformation in this phase under the bias voltage cannot be explained by the field induced devil's staircase. In this case a typical phase sequence FiLC(helical)→FiLC(unwound)→FLC(unwound) expected from the field induced devil's staircase can be FiLC(helical)→FiLC(distorted helical)→FLC(distorted helical)→FLC(unwound), since this sequence of transitions explains the results that have been obtained using a number of techniques given above.

ACKNOWLEDGMENTS

The authors thank Dr. A. J. Seed and Dr. M. Hird of the University of Hull, UK, for synthesizing the sample. Forbairt, Ireland, is acknowledged for supporting the research under its strategic program of research.

[1] L. A. Beresnev, L. M. Blinov, V. A. Baikalov, E. P. Pozhidaev, G. V. Parvanétskas, and A. I. Pavluchenko, Mol. Cryst. Liq. Cryst. **89**, 327 (1982).
[2] A. D. L. Chandani, E. Gorecka, Y. Ouchi, H. Takezoe, and A. Fukuda, Jpn. J. Appl. Phys. **28**, L1261 (1989); **28**, L1265 (1989).
[3] Ewa Gorecka, A. D. L. Chandani, Yu. Ouchi, H. Takezoe, and A. Fukuda, Jpn. J. Appl. Phys. **29**, L131 (1990).
[4] H. Orihara and Yo. Ishibashi, Jpn. J. Appl. Phys. **29**, L115 (1990).
[5] B. Žekš and M. Čepič, Liq. Cryst. **14**, 445 (1993).
[6] V. L. Lorman, A. A. Bulbitch, and P. Toledano, Phys. Rev. E. **49**, 1367 (1994).
[7] P. Bak and R. Bruinsma, Phys. Rev. Lett. **49**, 249 (1982).
[8] M. Yamashita and S. Miyazima, Ferroelectrics **148**, 1 (1993).
[9] A. Fukuda, Yo. Takanishi, T. Isozaki, K. Ishikawa, and H. Takezoe, J. Mater. Chem. **4**, 997 (1994).
[10] J. Hatano, Y. Hanakai, H. Furue, H. Uehara, S. Saito, and K. Murashiro, Jpn. J. Appl. Phys. **33**, 5498 (1994).
[11] Isa Nishiyama and J. W. Goodby (unpublished).
[12] Yu. Panarin, H. Xu, S. T. Mac Lughadha, J. K. Vij, A. J. Seed, M. Hird, and J. W. Goodby, J. Phys. Condens. Matter **7**, L351 (1995).
[13] S. Hiller, S. A. Pikin, W. Haase, J. W. Goodby, and Isa Nishiyama, Jpn. J. Appl. Phys. **33**, L1096 (1994).
[14] V. M. Vaksman and Yu. P. Panarin, Mol. Matter **1**, 147 (1992).
[15] K. Hiraoka, H. Takezoe, and A. Fukuda, Ferroelectrics **147**, 13 (1993).
[16] S. Hiller, S. A. Pikin, W. Haase, J. W. Goodby, and Isa Nishiyama, Jpn. J. Appl. Phys. **33**, L1170 (1994).
[17] K. Hiraoka, A. Taguchi, Yu. Ouchi, H. Takezoe, and A. Fukuda, Jpn. J. Appl. Phys. **29**, L103 (1990).
[18] M. Cepic, G. Heppke, J.-M. Hollidt, D. Lötzsch, and B. Žekš, Ferroelectrics **147**, 159 (1993).
[19] K. Hiraoka, Yo. Takanishi, K. Skarp, H. Takezoe, and A. Fukuda, Jpn. J. Appl. Phys. **30**, L1819 (1992).
[20] J. W. O'Sullivan, Yu. P. Panayin, J. K. Vij, A. J. Seed, M. Hird, and J. W. Goodby, J. Phys. Condens. Matter **8**, L551 (1996).